Available online at www.sciencedirect.com
SCIENCE DIRECT®
Journal of the European Ceramic Society 25 (2005) 935–941
www.elsevier.com/locate/jeurceramsoc

Internal friction investigation of phase transformation in nearly stoichiometric $LaMnO_{3+\delta}$

R. Zenati [a], C. Bernard [b], C. Calmet [b], S. Guillemet [b], G. Fantozzi [a], B. Durand [b,*]

[a] *Groupe d'Etudes de Métallurgie Physique et de Physique des Matériaux, GEMPPM 502, INSA de Lyon, 20 Av. A. Einstein, 69621 Villeurbanne Cedex, France*
[b] *Centre Interuniversitaire de Recherche et d'Ingénierie des Matériaux, CIRIMAT UMR 5085, Université Paul Sabatier, Bât. 2R1, 118 route de Narbonne, 31062 Toulouse Cedex 4, France*

Received 16 November 2003; received in revised form 4 March 2004; accepted 13 March 2004
Available online 20 June 2004

Abstract

Rhombohedral $LaMnO_{3+\delta}$ powders, prepared by two different soft chemistry routes (co-precipitation and hydrothermal synthesis), are sintered at 1400 °C for 2 h in air. Measurements of internal friction $Q^{-1}(T)$ and shear modulus $G(T)$, at low frequencies from −180 to 700 °C under vacuum, evidence three structural transitions of nearly stoichiometric orthorhombic $LaMnO_{3+\delta}$. The first one, at 250 or 290 °C, depending on the processing followed, is associated to either a Jahn–Teller structural transition or a phase transformation from orthorhombic to pseudo-cubic. The second one at 610 or 630 °C is related to a phase transformation from pseudo-cubic or orthorhombic to rhombohedral. Below the Neel temperature, around −170 °C, a relaxation peak could be associated, for samples prepared according to both processing routes, to the motion of Weiss domains.

Keywords: $LaMnO_3$; Internal friction; Phase transformation

1. Introduction

Manganese oxides $A_{1-x}B_xMnO_{3+\delta}$ (A = trivalent rare-earth; B = divalent metal such as Ca, Sr, Ba, or Pb) with perovskite structure have generated a great interest, especially since the discovery of colossal magnetoresistance (CMR).[1,2] Moreover, these oxides display prominent catalytic activity in many reactions,[3,4] including total oxidation of hydrocarbons and of volatile organic compounds.[5] Furthermore, they are attractive for environmental issues as cathode materials in solid oxide fuel cells.[6,7]

Various methods have been tested to synthesize the lanthanum manganite $LaMnO_{3+\delta}$ including the conventional solid-state reaction,[8] co-precipitation,[9,10] sol–gel[11] and molten salts reactions.[12] The literature is scarce on hydrothermal synthesis. Ovenston and Ponton[13] reported the preparation of lanthanum manganite mainly from acetate precursors in hydrothermal media adjusted at basic pH. Consequently, we have reinvestigated the hydrothermal synthesis of $LaMnO_{3+\delta}$ manganites studying the influence of several parameters, particularly that of complexing agents, such as citric acid.[14] A number of detailed investigations has shown that the synthesis temperature[14–17] and the oxygen partial pressure[18] control the Mn^{3+}/Mn^{4+} ratio in $LaMnO_{3+\delta}$ oxides.

The magnetic phase transitions are well known in these compounds.[19] Two additional structural transitions have been evidenced above room temperature.[20,21] The temperature of these transitions apparently depends on the initial Mn^{3+}/Mn^{4+} ratio.

The internal friction technique or "mechanical spectroscopy" is a very sensitive tool for studying phase transitions. Only a few studies have been done on the La/Mn/O system. Data have been found on "self-doped" $La_{0.8}MnO_3$ materials,[22] on $La_{0.82}Sr_{0.18}MnO_3$,[23] and on $La_{2/3}Sr_{1/3}MnO_3$,[24] but all these materials were prepared from solid-state reactions. This paper deals with the investigation, by mechanical spectroscopy, of some physical properties of lanthanum manganite ceramics obtained by sintering of $LaMnO_{3+\delta}$ nanometric powders, prepared using two different soft chemistry processes, co-precipitation and hydrothermal synthesis.

* Corresponding author. Tel.: +33-561-556140; fax: +33-561-556163.
E-mail address: bdurand@chimie.ups-tlse.fr (B. Durand).

0955-2219/$ – see front matter © 2004 Published by Elsevier Ltd.
doi:10.1016/j.jeurceramsoc.2004.03.015

2. Experimental

The powder morphology was observed by transmission electron microscopy (TEM, JEOL 2010 microscope) and the surface of ceramic compacts by scanning electron microscopy (SEM, JEOL JSM-35 CF microscope). The thermal decomposition of the precursors was examined by thermogravimetric and differential thermal analyses (TGA/DTA SETARAM TAG 24 thermoanalyzer, accuracy $<10^{-6}$ g). The structure was determined by X-ray diffraction analysis: the powder X-ray diffraction (PXRD) data were collected with a SEIFERT XRD-3003-TT diffractometer using the Cu-K_α radiation ($\lambda = 1.5418$ Å). Inductively coupled plasma (ICP) spectroscopy was used to determine the chemical composition of the oxides. The specific surface area was estimated by means of a Micromeritics Accusorb 2100E apparatus, defined by the Brunauer, Emmet and Teller (BET) method.

The accurate oxygen content was measured by temperature-programmed desorption analyses (TPD), involving thermogravimetry, gas chromatography and mass spectroscopy. The sample was first outgassed (1 Pa), at room temperature for 1 h, and then the system was filled with Ar. A flow of 15 $cm^3\,min^{-1}$ was allowed to run across the reactor. During the experiment, the temperature was linearly increased (rate of 5 °C min^{-1}). Every 120 s, the gas flowing out of the reactor was sampled and analyzed by gas chromatography (SHIMADZU GC-8A chromatograph fitted with a molecular column and a thermal conductivity detector). These analyses provided the oxygen concentration in the flowing gas, and the integration of these data over time gave the total amount of oxygen released during the experiment.

For physical investigations, lanthanum manganite powders were consolidated by uniaxial pressing up to 50 MPa. The green compacts were sintered at 1400 °C for 2 h in air, at a heating rate of 5 °C min^{-1}. The cooling was not controlled. The apparent density was measured by immersion in distilled water.[25] The shear modulus G and the mechanical losses Q^{-1} versus temperature were measured in the frequency range, 0.1–1.0 Hz, using a inverted torsion pendulum with maximum strain amplitude of 5×10^{-5}, under vacuum between −180 and 25 °C for low-temperature internal friction and room temperature and 700 °C for high-temperature internal friction, at a heating rate of 1 °C min^{-1}. The samples were rectangular bars of dimensions 40 mm × 4 mm × 1 mm. The sample was gripped at its extremities and twisted upon around the longitudinal vertical axis. The dynamic modulus was expressed according to relation:

$$G^* = G\exp(i\varphi) = G' + iG''$$

φ is the lag angle between the strain imposed and the resulting stress.

The mechanical losses versus temperature $Q^{-1}(T)$ were given by the ratio G'/G'' and the shear modulus $G(T)$ was equal to G'.

The phase transitions of lanthanum manganite were investigated using a diffractometer Siemens D5000 equipped with a heating camera Anton Parr (HTK10) and a linear detector Elphyse. The heating element was the platinum sample holder. The heating rate was 5 °C min^{-1} and the patterns were recorded under vacuum at various temperatures after a dwell for 30 min at the considered temperature.

3. Powder preparation and characterization

3.1. Hydrothermal synthesis

When carried out in appropriate conditions, the hydrothermal treatment, performed at 150 °C for 20 h under autogenous pressure, of aqueous media containing lanthanum nitrate, manganese(II) nitrate and citric acid at the same concentration (0.28 mol L^{-1}) and ammonia for pH adjustment, leads to amorphous precursors of $LaMnO_{3+\delta}$ powders. Their pyrolysis has been investigated by wide angle X-ray scattering.[26] The preparation procedure and the characteristics of the lanthanum manganite powders, obtained by pyrolysis at 800 °C under air, had been previously published.[14]

The annealing of the amorphous precursor at 800 °C under air for 2 h allows to remove most of the residual carbon (<0.5 wt.%) and to obtain the rhombohedral perovskite phase (Fig. 1) with the $R\bar{3}c$ space group. The XRD patterns reveal only the perovskite-type structure.

The average crystallite size, calculated from broadening of the XRD peaks using the Scherrer formula for a spherical model, is 45 nm. The TEM observation (Fig. 2) shows more or less spherical crystallites with sizes in the range 30–50 nm. The mean size estimated from the measurement of the size of 50 crystallites, 40 nm, is close to that calculated from XRD peak broadening. The analysis of the lanthanum manganite powders by EDX shows a homogeneous chemical composition. The atomic ratio La/Mn = 1.03 is in good agreement with the one obtained from chemical

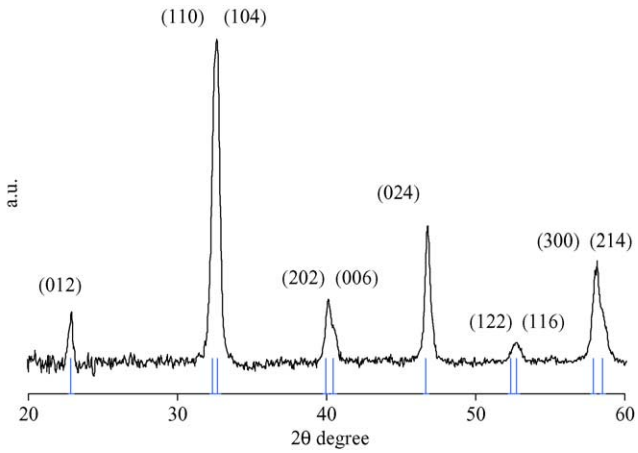

Fig. 1. XRD pattern of lanthanum manganite powders obtained by hydrothermal treatment at 150 °C for 20 h and annealed at 800 °C for 2 h.

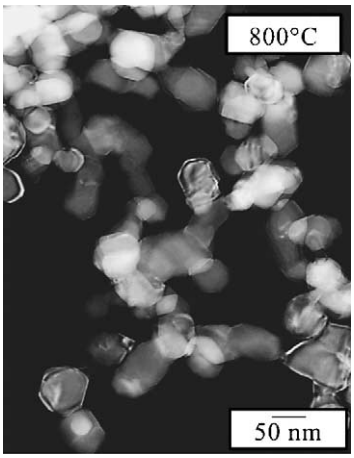

Fig. 2. TEM micrograph of the powder obtained by hydrothermal treatment and annealed at 800 °C for 2 h.

analysis (1.02). It is noticed that the hydrothermal synthesis allows to obtain a non-stoichiometry coefficient δ of 0.145 for the sample annealed at 800 °C under air for 2 h, which corresponds to 29% of Mn^{4+}.

After sintering at 1400 °C under air for 2 h, the dense ceramics (Fig. 3) show no open porosity and no micro-cracking. The grain size is in the range 5–10 μm and the apparent density is about 6.4. The sintering decreases the non-stoichiometry coefficient up to $\delta = 0.02$ and induces the phase transformation from rhombohedral to orthorhombic.

3.2. Coprecipitation via the citrate route

This method, first developed by Szabo,[27] allows to obtain mixed oxides with the perovskite structure at moderate temperature. The synthesis of the mixed citrate requires first to prepare the lanthanum, strontium and manganese simple citrates. Lanthanum and strontium citrates are obtained according to the following procedure. 0.2 mol of the corresponding nitrates is dissolved in 600 ml of water. The solution is poured in an aqueous solution of di-ammonium hydrogen citrate and stirred for 1 h. The obtained precipitate is separated from the liquid phase by centrifugation. Thermogravimetric analyses show that the two citrates have the respective formula: $La(C_6H_5O_7)\cdot 3.5H_2O$ and $Sr_3(C_6H_5O_7)_2\cdot 3.5H_2O$. A different procedure is used for the synthesis of manganese citrate. A solution containing 0.5 mol of MnO_2 is poured in an aqueous solution containing 0.5 mol of citric acid $C_6H_8O_7\cdot 6H_2O$. According to Szabo,[27] intermediate Mn^{4+} ions are formed and can oxidize citric acid into acetone. The resulting Mn^{3+} ions reacts with the excess of citric acid to form the insoluble citrate, $Mn(C_6H_5O_7)\cdot H_2O$. The mixed La–Sr–Mn citrate is obtained after the dissolution of the simple citrates in a hot ammoniacal solution. The solution is then evaporated and the solid grinded.

The lanthanum and manganese molar contents, determined from ICP method, are, respectively, 0.99 and 1.01. TGA and TPD analyses show that the heating of the mixed citrate leads to a dehydration and to a release of CO and CO_2.[9] Its decomposition into oxide is complete above 530 °C. In order to compare the characteristics of $LaMnO_3$ powders prepared by the two different ways (hydrothermal and citrate method), the powder was annealed at 700 °C for 2 h in air. TEM observations show that the powder is constituted of crystallites of approximately 30 nm (Fig. 4). X-ray diffraction analysis reveals that the structure exhibits rhombohedral symmetry with the $R\bar{3}c$ space group (Fig. 5). The non-stoechiometry coefficient of the powder, $\delta = 0.14$, and the density after sintering under air at 1400 °C for 2 h, $d = 6.4$, are similar to the ones obtained for hydrothermal powders. On the contrary, the non-stoichiometric coefficient of the sintered pellet, $\delta = 0.08$, is higher than that of the pellet prepared from hydrothermal powder, $\delta = 0.02$. The irreversible phase transformation from rhombohedral to orthorhombic also occurs during the sintering in air.

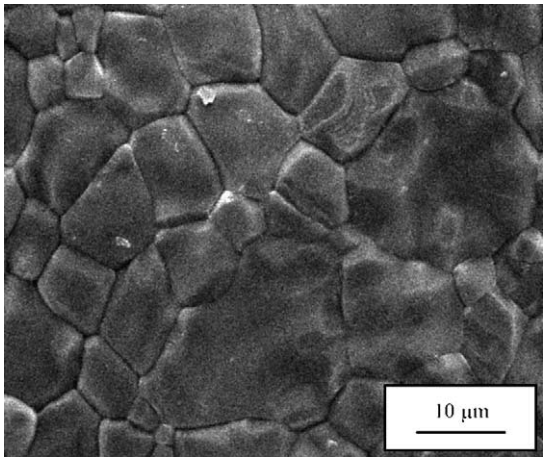

Fig. 3. SEM observation of a ceramic surface sintered at 1400 °C for 2 h.

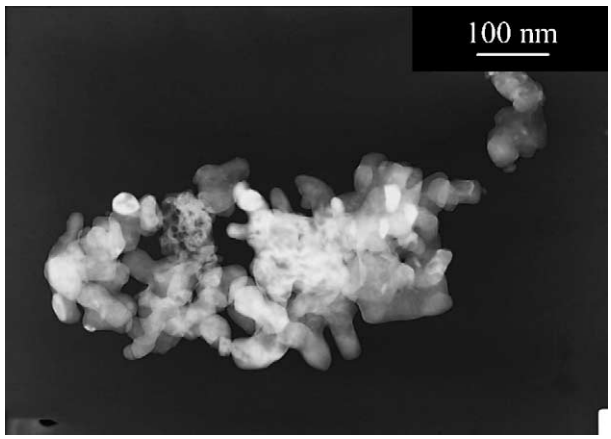

Fig. 4. TEM micrograph of an ex-citrate $LaMnO_{3+\delta}$ oxide treated at 700 °C.

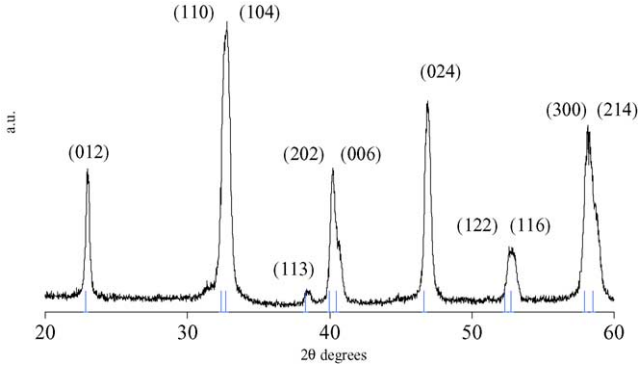

Fig. 5. XRD pattern of an ex-citrate $LaMnO_{3+\delta}$ oxide treated at 700 °C.

4. Internal friction measurement results

Measurements of the internal friction $Q^{-1}(T)$ and shear modulus $G(T)$ of $LaMnO_3$ at low frequencies (0.1, 0.3, 1.0 Hz) from room temperature to 700 °C, show two damping peaks P_1 and P_2, situated around 270 and 620 °C, respectively, and their correlated minimum modulus A_1 and A_2 (Fig. 6), that indicate two transitions above room temperature.[28] Detailed analysis of the data situates more accurately a transition at $T_1 = 290$ °C and another at $T_2 = 630$ °C for the powder obtained via hydrothermal synthesis (Fig. 7) and at $T_1 = 250$ °C and $T_2 = 610$ °C for the powder obtained via the citrate route (Figs. 6 and 7).

The overall internal friction behavior of the lanthanum manganite above room temperature does not appear sensitive to the method of powder preparation, apart from the fact that the peaks from $LaMnO_{3+\delta}$ powder obtained via hydrothermal synthesis are shifted toward slightly higher temperatures (Fig. 7).

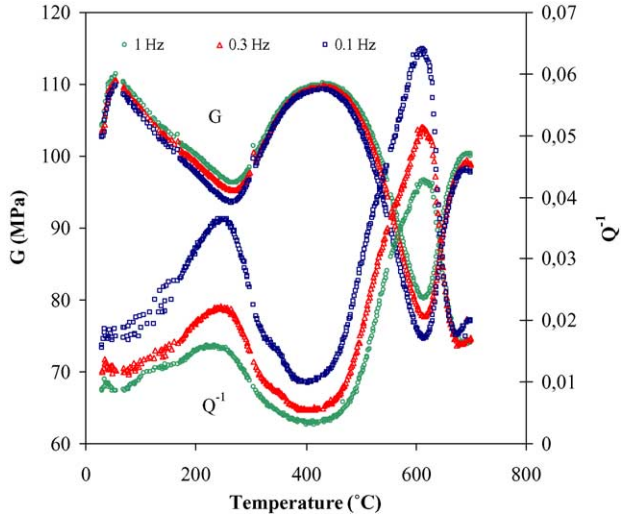

Fig. 6. Mechanical losses and associated shear modulus versus temperature (high temperature): sample processed from powders obtained via citrate route.

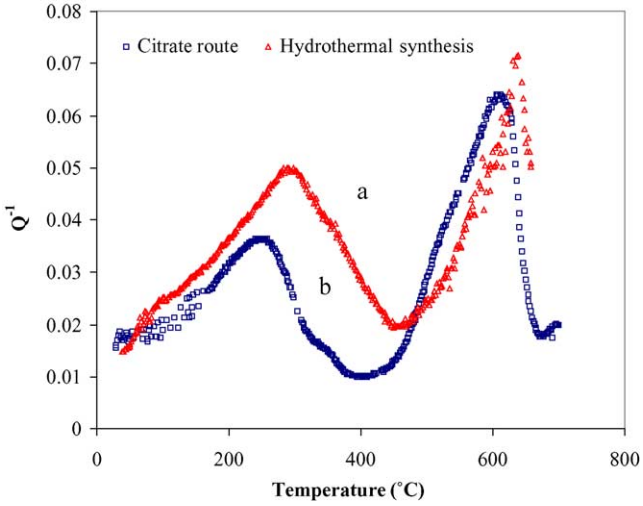

Fig. 7. Mechanical losses vs. temperature: (a) sample processed from powders obtained via hydrothermal synthesis and (b) sample processed from powders obtained via citrate route.

For these two internal friction peaks, it is noticeable that, while the peak temperature does not change, the height of the peak increases as the frequency decreases.

At low temperature, the mechanical losses curve $Q^{-1}(T)$ shows a peak R near −170 °C associated with a significant slope change in the decrease of elastic modulus versus temperature ($G(T)$), as shown in Fig. 8 for the sample prepared by hydrothermal synthesis. The peak temperature is below the Neel temperature (−113 °C[29]). Its height is independent of the frequency, but the mechanical losses and the elastic modulus are shifted toward higher temperatures when the frequency is increased.

The XRD patterns indicate that for both samples, at 750 °C under vacuum, the lanthanum manganese oxide exhibits a rhombohedral structure and that after cooling at

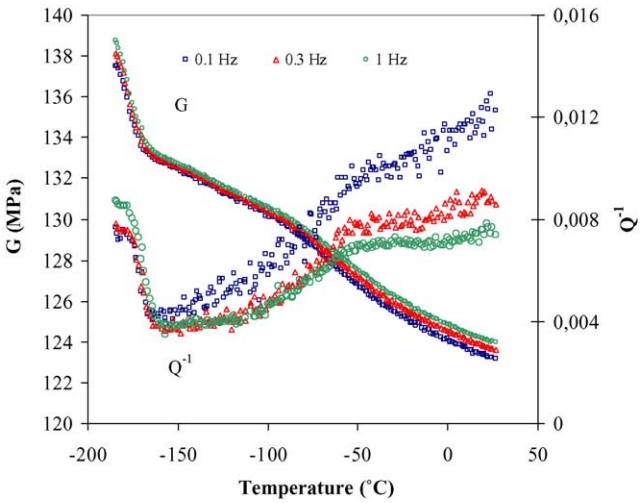

Fig. 8. Mechanical losses and associated shear modulus vs. temperature (low temperatures): sample processed from powders obtained via hydrothermal route.

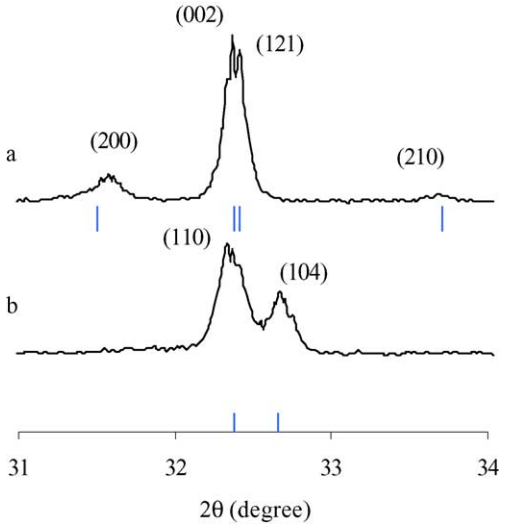

Fig. 9. High-temperature X-ray diffraction profiles for $LaMnO_{3+\delta}$, orthorhombic phase at low temperature (a), i.e., ambient temperature under vacuum and rhombohedral phase at high temperature (b), i.e., 750 °C under vacuum.

room temperature under vacuum the structure becomes orthorhombic as seen in Fig. 9 for the co-precipitated sample.

5. Discussion

Mechanical spectroscopy is an interesting tool for studying phase transitions or domain relaxations.[28] Internal friction and elastic modulus measurements have been made on doped manganites but rather in the low-temperature range.[22,24,30,31] These studies show that very often two peaks associated with a modulus softening appear at low temperature. These peaks are typical of a phase transition: indeed, they do not shift with frequency.[28] The low-temperature peak could be associated to a phase separation of an antiferromagnetic phase from the ferromagnetic matrix whereas the high-temperature internal friction peak can be due to the ferromagnetic-paramagnetic transition.

The evolution of the crystal structure of orthorhombic stoichiometric $LaMnO_3$ has been determined as a function of temperature by Norby et al.[20] first and more recently by Rodriguez-Carvajal et al.[21] The former prepared orthorhombic $LaMnO_3$ by heating rhombohedral $LaMnO_{3+\delta}$ ($\delta = 0.14$) at 900 °C under N_2 and cooling to room temperature under N_2. They indicated a composition corresponding to $La_{1.00}Mn^{III}_{0.99}Mn^{IV}_{0.01}O_{3.005}$. Then, using high-temperature X-Ray powder diffraction, they investigated the thermal transformation of orthorhombic $LaMnO_3$ under nitrogen and observed two transitions: the transition from orthorhombic to pseudo-cubic at ca. 327 °C and the transformation from pseudo-cubic to rhombohedral at ca. 527 °C. For the intermediate pseudo-cubic phase, the unit cell parameter is twice the one of the ideal cubic perovskite structure. The study by neutron powder diffraction at variable temperature showed that the Jahn–Teller distortion, found in the orthorhombic room temperature phase, is not seen in the high-temperature rhombohedral phase where all Mn–O distances are equal. The latter prepared pure orthorhombic $LaMnO_3$ by crushing single crystals grown by the floating zone method and, studying the thermal behavior under vacuum, they observed two transitions at, respectively, 477 and 737 °C, i.e., at temperatures significantly higher than Norby et al.[20] The gap was interpreted by the presence of a non-negligible amount of Mn^{4+} in the sample of reference 20. From Rietveld crystal structure refinement, the authors concluded that the transition at 477 °C corresponds to the disappearance of the cooperative Jahn–Teller effect responsible of the orthorhombic distortion below 477 °C. Between 477 and 737 °C, the XRD patterns could be indexed assuming, either a double cubic perovskite cell as Norby et al.[20] or an orthorhombic cell (O′). However, the true symmetry of this phase was still orthorhombic because the Bragg intensities could not be explained within any of the possible cubic space groups, whereas the space groups *Pbnm* of the room temperature orthorhombic phase (O) worked perfectly. The second transition at 737 °C was attributed to the phase transition from the intermediate temperature orthorhombic phase (O′) to the high-temperature rhombohedral phase already characterized in reference 20.

Above room temperature, our results of mechanical spectroscopy show very clearly the presence of two peaks P_1 and P_2 situated around 250 and 610 °C, respectively. Their features (peak temperature independent of frequency, decreasing of peak height with increasing frequency) are characteristic of a phase transition. These two peaks are associated with minima of elastic modulus A_1 and A_2; it can be noticed that the curve elastic modulus as a function of temperature begins to deviate from the normal variation before the minima A_1 and A_2 (near the temperature of the peaks P_1 and P_2).

In agreement with Norby et al.[20] and Rodriguez-Carvajal et al.[21], the shift of the temperature of peaks P_1 and P_2 between the hydrothermal and the co-precipitated pellets is due to the presence of Mn^{4+} in nearly stoichiometric $LaMnO_{3+\delta}$; the lower the temperature of the peaks, the higher the Mn^{4+} content (Table 1). In this diagram, the value given by Norby et al.[20] seems unusually low. Following the same authors, two hypothesis can be proposed for the peak P_1: either a Jahn–Teller structural transition due to the disappearance of

Table 1
Influence of the Mn^{4+} content on the temperatures of phase transition in $LaMnO_{3+\delta}$

Formula	T_1 (°C)	T_2 (°C)
$LaMnO_3$[21]	477	737
$La_{1.00}Mn^{3+}_{0.99}Mn^{4+}_{0.01}O_{3.005}$[20]	327	527
$La_{1.00}Mn^{3+}_{0.96}Mn^{4+}_{0.04}O_{3.02}$ pellet ex hydrothermal powder	290	630
$La_{1.00}Mn^{3+}_{0.84}Mn^{4+}_{0.16}O_{3.08}$ pellet ex co-precipitated powder	250	610

orbital ordering, the phase remaining orthorhombic above T_1 as proposed by Rodriguez-Carvajal,[21] or to a phase transformation from orthorhombic to pseudo-cubic as proposed by Norby et al.[20] The peak P_2 can be attributed to the phase transition either from pseudo cubic to rhombohedral as proposed by Norbyet al.[20] or from orthorhombic to rhombohedral as proposed by Rodriguez-Carvajal.[21] Based on the available information, one cannot discriminate between the two possibilities.

The features of the peak R (height independent of the frequency, internal friction and elastic modulus shifted toward higher temperatures as the frequency is increased), appearing at low temperature near $-173\,^{\circ}C$, with the classical associated decrease of modulus, are characteristic of a relaxation peak.[28] This relaxation peak situated below the Neel temperature ($T_N = -113\,^{\circ}C$) could be associated to the motion of Weiss domains by analogy with the ferroelectric behavior.[28] But this hypothesis must be confirmed by further experiments.

6. Conclusion

In orthorhombic nearly stoichiometric $LaMnO_{3+\delta}$ pellets, obtained by sintering in air of hydrothermally prepared and co-precipitated powders, three internal friction manifestations have been revealed. The first one, a relaxation peak below the Neel temperature, could be associated to the motion of Weiss domains. The second and the third ones are evidenced by two internal friction peaks associated to minima of elastic modulus. They are attributed to phase transitions previously studied by XRD and neutron diffraction at high temperature.[20,21] According to the authors, the two following sequences could be proposed:

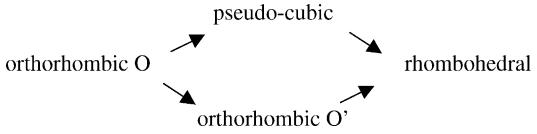

The interest of mechanical spectroscopy is all the more significant, as we have not been able to reveal the existence of the two phase transitions neither by differential thermal analysis, nor by differential scanning calorimetry.

References

1. Steenbeck, K., Eick, T., Kirsch, K., Schmidt, H. G. and Steinbeiss, E., C.M.R. sensors for room temperature applications. *Appl. Phys. Lett.* 1998, **73**, 2506–2508.
2. De Andrés, A., García-Hernández, M., Muñoz-Martín, A., Martín, L., Prieto, C., Calzada, L. *et al.*, Influence of the microstructure on the magnetoresistance of manganite thin films. *Superficies y Vacío* 1999, **9**, 143–146.
3. Nitadori, T., Kurihara, S. and Misono, M., Catalytic properties of $La_{1-x}A'_xMnO_3$ ($A' = Sr, Ce, Hf$). *J. Catal.* 1986, **98**, 221–228.
4. Tanaka, H., Mizuno, N. and Misono, M., Catalytic activity and structural stability of $La_{0,9}Ce_{0,1}Co_{1-x}Fe_xO_3$ perovskite catalysts for automotive emissions control. *Appl. Catal. A* 2003, **6461**, 1–12.
5. Blasin-Aubé, V., Belkouch, J. and Monceaux, L., General study of catalytic oxidation of various V.O.C.s over $La_{0,8}Sr_{0,2}MnO_{3+x}$ perovskite catalyst – influence of mixture. *Appl. Catal. B* 2002, **1329**, 1–12.
6. Anderson, H. U., Review of p-type perovskite materials for S.O.F.C. and other applications. *Solid State Ionics* 1992, **52**, 33–41.
7. Prigent, M., *Les piles à combustibles*, Institut français du pétrole, 1997.
8. Hammouche, A., Siebert, E. and Hammou, A. M., Crystallographic, thermal and electrochemical properties of the system $La_{1-x}Sr_xMnO_3$ for high temperature solid electrolyte fuel cells. *Mater. Res. Bull.* 1989, **24**, 36.
9. Guillemet-Fritsch, S., Coradin, H., Barnabé, A., Calmet, C., Tailhades, Ph. and Rousset, A., Advances in the low temperature preparation and structural characterization of lanthanum strontium manganite powder. *Mater. Res. Soc. Symp. Proc.* 2001, **674**, U331–U336.
10. Maurin, I., Barboux, P., Lassailly, Y. and Boilot, J. P., La(Sr,Pb)MnO_3 thin films through solution techniques. *Chem. Mater.* 1998, **10**, 1727–1732.
11. Gaudon, M., Laberty-Robert, C., Ansart, F., Stevens, P. and Rousset, A., Preparation and characterization of $La_{1-x}Sr_xMnO_{3+\delta}$ ($0 \leq x \leq 0,6$) powder by sol–gel processing. *Solid State Sci.* 2002, **4**, 125–133.
12. Ciaravino, C., Lyonnet, R., Scharff, J. P., Durand, B. and Deloume, J. P., Reactivity in molten oxonitrate of lanthanum and manganese salts. Synthesis of $La_{1-x}MnO_3$. *J. High Temp. Mater. Processes* 1999, **3**(2), 269–278.
13. Ovenston, J. and Ponton, C. B., Hydrothermal synthesis and characterization of strontium doped lanthanum manganite perovskite powders for use as a cathode in material in S.O.F.C.. *Br. Ceram. Proc.* 1998, **58**, 155–164.
14. Bernard, C., Laberty, C., Ansart, F. and Durand, B., Hydrothermal synthesis of $La_{1-x}Sr_xMnO_{3+\delta}$ manganites. *Annales de chimie Science des Matériaux* 2003, **28**, 85–86.
15. Topfer, J. and Goodenough, J. B., $LaMnO_{3+\delta}$ revisited. *J. Solid State Chem.* 1997, **130**, 117–128.
16. Mizusaki, J., Mori, N., Takai, H., Yonemura, Y., Minamiue, H., Tagawa, H. *et al.*, Oxygen nonstoichiometry and defect equilibrium in the perovskite-type $La_{1-x}Sr_xMnO_{3+\delta}$. *Solid State Ionics* 2000, **129**, 163–177.
17. Verelst, M., Rangavittal, N., Rao, C. N. R. and Rousset, A., Metal-insulator transitions in anionexcess $LaMnO_{3+\delta}$ controlled by the Mn^{4+} content. *J. Solid State Chem.* 1993, **104**, 74–80.
18. Kuo, J. H., Anderson, H. U. and Sparlin, M., Oxidation-reduction behavior of undoped and Sr-doped $LaMnO_3$ non-stoichiometry and defect structure. *J. Solid State Chem.* 1989, **83**, 52–60.
19. Alonso, J. A., Martinez-Lope, M. J., Casais, M. T. and Munoz, A., Magnetic structure of $LaMnO_{3+\delta}$ perovskites. *Solid State Commun.* 1997, **102**(1), 7–12.
20. Norby, P., Krogh Andersen, I. G. and Krogh Endersen, E., The crystal strcuture of lanthanum manganate(III) $LaMnO_3$ at room temperature and 1273 K under N_2. *J. Solid State Chem.* 1995, **119**, 191–196.
21. Rodriguez-Carvajal, J., Hennion, M., Moussa, F., Pinsard, L. and Revcolevschi, A., The Jahn–Teller structural transition in stoichiometric $LaMnO_3$. *Physica B* 1997, **234–236**, 848–850.
22. Zheng, L. Q. and Fang, Q. F., Internal friction study of phase transition in self-doping $La_{0,8}MnO_3$ bulk materials. *J. Phys. Condens. Mater.* 2001, **13**, 1–8.
23. Li, H. Q., Fang, Q. F., Yin, W. H. and Zhu, Z. G., The internal friction and electrical and magnetic properties of $La_{0.82}Sr_{0.18}MnO_3$ bulk materials. *Scripta Materialia* 2002, **46**, 691–694.
24. Seiro, S., Ghilarducci, A., Salva, H., Vasquez Mansilla, M., Saint Paul, M., Lejoy, P. *et al.*, High temperature elastic measurements in $La_{2/3}Sr_{1/3}MnO_3$ at low frequency. *J. Magn. Magn. Mater.* 2001, **226–230**, 988–989.

25. Arthur, G., *J. Instr. Met*. 1954, **83**, 329–336.
26. Bernard, C., Durand, B., Verelst, M. and Lecante, P., Hydrothermal synthesis of $LaMnO_{3+\delta}$?: F.T.I.R. and W.A.X.S investigations of the evolution from amorphous to crystallized powder. *J. Mater. Sci*. 2004, **281**, 2821–2826.
27. Szabo, G., *Contribution à l'étude des aluminates, manganites et ferrites de terres rares et d'Yttrium*, Thesis, Lyon, 1969.
28. Schaller, R., Fantozzi, G. and Gremaud, G., *Mechanical Spectroscopy Q^{-1} 2001*. Trans. Tech. Publications, Switzerland, 2001.
29. Van Roosmalen, J. A. M. and Corfunke, E. H. P., The defect chemistry of $LaMnO_{3+\delta}$. *J. Solid State Chem.* 1994, **110**, 100–115.
30. Wang, G. T. and Fang, Q. F., Low temperature internal friction study of phase transition of $La_{0.95}K_{0.05}MnO_3$ bulk materials. *Phys. Stat. Sol (a)* 2002, **191**(1), 260–266.
31. Li, H. Q., Fang, Q. F. and Zhu, Z. G., The low frequency internal friction and electric magnetic properties in $La_{0.7}Pb_{0.3}MnO_3$ bulk materials. *Mater. Sci. Eng.* 2004, **A370**, 388–391.